THE UNIVERSITY *of* EDINBURGH

Edinburgh Research Explorer

Optimal collaborative demand-response planner for smart residential buildings

OPEN ACCESS

Optimal Collaborative Demand-Response Planner for Smart Residential Buildings

Juan A. Gomez-Herrera[a,*], Miguel F. Anjos[a]

[a]*GERAD and Department of Mathematics and Industrial Engineering, Polytechnique Montreal, C.P. 6079, Succ. Centre-Ville, Montreal, QC, Canada H3C 3A7.*

Abstract

This work presents a collaborative scheme for the end-users in a smart building with multiple housing units. This approach determines a day-ahead operational plan that provides demand-response services by taking into account the amount of energy consumed per household, the use of shared storage and solar panels, and the amount of shifted load. We use a biobjective optimization model to trade off total user satisfaction versus total cost of energy consumption. The optimization works in combination with a price structure based on time and level of use that encourages load shifting and benefits the participants. Computational experiments and an extensive sensitivity analysis validate the performance of the proposed approach and help to clarify its strengths, its limits, and the requirements for ensuring the desired outcome.

Keywords: Smart Buildings, Demand-Response, Residential Load, Biobjective Optimization, Compromise Programming.

1. Notation

Sets:

$i \in I$: Energy levels
$j \in J$: Users
$t \in T$: Time frames

Parameters:

D_{jt} : Energy demand of user j in time frame t (kWh)
K_{it} : Price per energy unit bought from the grid in level i in time frame t (¢/kWh)
C^L : Available capacity in the lower level (kW)
C_j^H : Available capacity in the higher level for user j (kW)
B : Cost of charging the battery per energy unit (¢/kWh)
S^{max} : Capacity of the battery (kWh)
Γ : Battery efficiency
Z : Number of cycles allowed in the battery
P_t : Incentive paid by the grid per energy unit in a demand-response call in time frame t (¢/kWh)
DR_t : Energy consumption reduction requested by the grid in time frame t (KWh)
G_t^{max} : Available energy from solar panels in time frame t (¢/kWh)
F : Cost per energy unit obtained from the solar panels (¢/kWh)

Y_j : Max accumulated shifted demand over the horizon accepted by user j (kWh)
$\hat{Y}_j$: Max unmet demand at the end of the horizon for user j (kWh)
Ψ_{sol}^{max} : Max percentage of total demand satisfied by solar panels
Ψ_{sol}^{min} : Min percentage of total demand satisfied by solar panels
Ψ_{bat}^{max} : Max percentage of total demand satisfied by the battery
Ψ_{bat}^{min} : Min percentage of total demand satisfied by the battery

Variables:

x_{ijt} : Energy bought from the grid in level i by user j in time frame t
y_{jt} : Accumulated unmet demand at the end of period t for user j
soc_{jt} : Individual state of charge for user j at the end of time frame t
s_{jt}^+ : Energy charged in the battery in time frame t by user j
s_{jt}^- : Energy discharged from the battery in time frame t by user j
r_{jt} : Amount of demand-response service provided by user j in time frame t
g_{jt} : Consumed energy from solar panels for user j in time frame t

---

*Corresponding author
Email address:* `juan.gomez@polymtl.ca` (Juan A. Gomez-Herrera)

$$\alpha_t \quad : \quad \begin{cases} 1 & \text{Battery charges during time frame } t \\ 0 & \text{Battery discharges during time frame } t \end{cases}$$

$$z_t \quad : \quad \begin{cases} 1 & \text{Battery changes from charging to discharging or vice versa} \\ 0 & \text{Otherwise} \end{cases}$$

$$\phi_t \quad : \quad \begin{cases} 1 & \text{The building agrees to provide demand response in time frame } t \\ 0 & \text{Otherwise} \end{cases}$$

2. Introduction

The implementation of smart buildings introduces two major challenges for consumer planning. First, consumers desire to meet their energy requirements keeping a high level of satisfaction at a minimum cost. These objectives can rarely be attained simultaneously. Second, the energy supplier (system operator, utility, etc.) is required to meet user demand while ensuring system stability. It is often expensive to satisfy these requirements during peak consumption times.

The end-users play an important role in the mission of balancing generation and demand. This participation is driven mainly by a) demand response (DR), defined as "changes in electric usage by demand-side resources from their normal consumption patterns in response to changes in the price of electricity over time, or to incentive payments designed to induce lower electricity use at times of high wholesale market prices or when system reliability is jeopardized " [1], and b) smart grids, which support communication and decision-making by both users and generators. These technologies also allow the integration of new resources, such as distributed generators, solar panels, and storage units, that increase the complexity of the system but may offer benefits to all the participants.

Traditionally DR pricing programs are offered to residential and commercial customers, while DR incentive-based programs are meant for large commercial and industrial consumers capable of provide significant load reduction, often in exchange for a financial incentive [2]. Nevertheless the residential and commercial sectors represent a major part of the total consumer demand [3], and the aggregated DR potential in these sectors could play an important role in the current and future operation of the grid. However it is difficult to exploit this potential due to the large number of consumers. An entity capable of coordinating the actions of multiple end-users can aggregate enough DR potential, not only to participate through pricing programs but also to provide DR services through incentive-based programs. The approach presented in this article aims to support and facilitate this coordination process.

Previous works have considered different aspects when treating this task. Typically they include single or multiple users, storage and/or distributed generation and they focus on the planning and control of the system. The approach in [4] schedules generators, storage devices, and controllable loads, and compensates for the uncertainties in the dynamics of the system through a model predictive control strategy.

A similar idea is explored in [5], including models for combined heat and power generation, in the presence of thermal and electrical loads and storage units. An economic comparison of a rolling-horizon approach and the standard unit commitment for microgrids is presented in [6].

The authors in [7] propose a robust optimal control to manage the load prediction uncertainty for cooling devices in a DR context. The algorithm presented in [8] schedules loads for large populations. It aggregates different types of appliances and distributed energy systems.

The mixed integer programs in [9] and [10] minimize the use of conventional generation resources in order to encourage the use of the batteries of electric vehicles and the available renewable resources, ensuring a high level of self-consumption. The approach presented in [11] assesses several configurations of a grid-connected microgrid, considering a two-way flow of power and its impact on the grid. An autonomous microgrid optimal operation approach is presented in [12], considering the generation and consumption sides and the balance between the two in a real-time scenario. A function based on declining block rates achieves a balance between user comfort and electricity cost in [13]. It presents a microeconomic analysis of this function, and the method is used for bidirectional energy trading.

All the approaches mentioned previously minimize the total operational cost. Cost is a popular and important performance measure, but even though it conveys important information, it neglects the perspective of user's satisfaction which is key in a DR context.

Other works take into account elements such as user comfort and preferences via constraints and/or costs that approximate the level of satisfaction. This way of dealing with conflicting objectives is one among several options in multiobjective optimization [14]. When objectives conflict, such as cost and comfort in our case, there is usually no solution that optimizes them simultaneously. To improve one of the objectives we may have to worsen one or more of the others. When this is the case, the solution is said to be Pareto efficient, Pareto optimal, or nondominated.

A comprehensive review of methods to find Pareto efficient solutions can be found in [15]. It presents approaches that include the user preferences in the decision-making and that represent and approximate the Pareto front (the set of Pareto efficient solutions).

Multiobjective optimization has been explored in the smart grid context. Particle swarm optimization and weighted aggregation are used in [16] to approximate the Pareto front for energy cost and environment comfort. The Pareto front is approximated using the ϵ-constraint method in [17], balancing the total cost and the energy obtained from

distributed generators in isolated sites, and in [18] and [19] minimizing both pollutant emission and operating cost.

Lexicographic goal programming is used in [20] to minimize the operational costs, the emissions produced, and the asset deterioration resulting from exposure to excess temperatures.

Finally, the weighted-sum approach is used to balance the minimization of load curtailment, operating cost, and pollutant emission in [21], and energy costs and thermal comfort in [22].

The same approach is used in [23] to trade off the operational cost of two buildings that share combined cooling and heating systems, battery and thermal storage. In this case the model ensures demand satisfaction at a minimum cost for the building cluster but does not consider other elements such as DR incentives, load shifting or renewable energy integration.

Although there is a growing interest in the trade-offs between conflicting objectives such as cost and user satisfaction, there is still the need to integrate these features in a DR context. Greater DR participation can be achieved through the coordination and aggregation of multiple consumers who will prioritize not only cost but also demand satisfaction.

This paper presents, to the best of our knowledge, the first framework for residential DR that includes two of the most common types of DR programs, namely incentive-based programs and pricing programs, while considering the user satisfaction via biobjective optimization.

Our approach determines an operational plan for a smart building with multiple housing units. The framework considers DR programs and balances cost and shifted load for the end-users. We use biobjective optimization to find efficient trade-offs between the two conflicting objectives without estimating the Pareto front. These are the main contributions of this article:

- We model the individual shifting capabilities of the user as a resource whose cost is handled via biojective optimization. In this scenario the consumers may actively participate, choosing when to shift load and to provide DR.

- We propose and analyse a novel pricing structure that encourages a more homogeneous consumption during the planning horizon.

- We propose a tool to optimally coordinate shared resources such as batteries and solar panels, keeping track of the individual usage and ensuring a fair allocation.

- We present a sensitivity analysis that provides insight into the selection and definition of parameters and their effect in the final result.

This paper is structured as follows. The proposed approach is described in Section 3, the computational experiments and sensitivity analysis are presented in Section 4, and the conclusion is given in Section 5.

3. Proposed Optimization Approach

Figure 1 shows the general operation of the smart building. The planning module is composed of a centralized energy management system with two-way communication with the households, the resources and the grid. This module receives day-ahead information from each household in the form of an energy demand forecast D_{jt} and shifting preferences Y_j and $\hat{Y}_j$. Each household can determine and transmit this information using a smart meter and its local energy management system.

It is important to highlight that the battery and a set of solar panels are managed by the planning module, and they are resources that are shared among all the housing units. Therefore, the module receives the current state of charge soc_{jt} from the battery, and the expected solar generation G_t^{max} from the solar panels. In addition, in the context of an incentive-based DR program, the planning module receives the scheduled DR requests from the grid.

Once all the information has been gathered, the planning module solves a biobjective optimization problem for the building, finding an optimal trade-off between the total cost and the shifted load. The shifted load represents the level of dissatisfaction perceived by the household, depending on its submitted preferences for when and by how much consumption can be delayed or reduced.
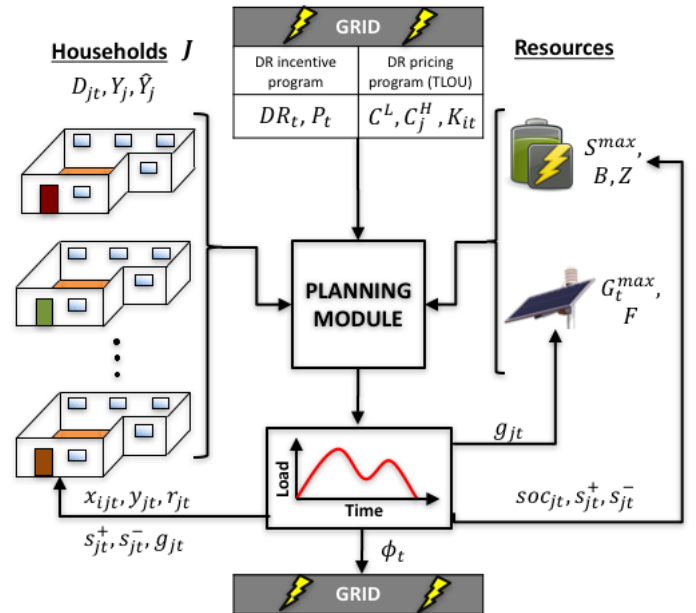

Figure 1: Smart building operation.

After solving the optimization problem, we obtain individual plans that specify, for each user and time frame, the amount of energy to be drawn from the grid x_{ijt}, the

allocation of the energy obtained from the solar panels g_{jt}, the use of the battery s_{jt}^+ and s_{jt}^-, and the shifted load y_{jt}.

We note that the technology required to implement the proposed scheme is commonly available in the modern context of the Internet of Things. A variety of smart meters, smart appliances, and smart thermostats enable two-way communication between the planning module and the households, the resources, and the grid, as depicted in Figure 1. A comprehensive review of the requirements for a successful implementation of this type of system is presented in [24].

One of the main features of this approach is that it finds a balance between total cost and shifted load while providing DR services. We include two of the most common types of DR: incentive-based programs and pricing programs. For the incentive-based program the optimization model decides whether or not the building answers a DR call. In the case of a positive answer, the building commits to lowering consumption by using the battery or allocating capacity reductions to some customers, who shift load accordingly. Finally, it reports to each household its share of the DR provided and the benefit obtained. The pricing program encourages peak reduction through the combination of different prices.

We include a *time and level of use (TLOU) pricing structure* in which the price varies time-wise and level-wise [25]. This is an extension of the time of use (TOU) pricing that is widely used. The TLOU pricing is represented by the parameter K_{it}. In each time frame t, each user can consume up to capacity i, paying price K_{it}. Beyond this threshold the user will pay the next price, $K_{i+1,t}$. We consider two pricing levels for each time frame, a *lower* price and a *higher* price, but in general several levels can be used. This pricing structure works in combination with the DR requests from the grid and the willingness to shift load. Its effect is strengthened via the use of the storage unit and solar panels. The costs associated with these two resources represent the amortization of the corresponding investments.

So far we have considered the main features and advantages of the proposed approach. We identify some limitations as well. As mentioned before, the approach considers the end-user perspective (cost and demand satisfaction), which means that it is not a method to directly control the peaks of consumption. Any peak reduction will come as a consequence of users' decisions (motivated by a combination of cost and satisfaction) and not from direct intervention by the utility. This aspect will be explored in Section 4.2 in which the proper selection of the cost structure by the utility facilitates the peak reduction. Additionally, the optimization model only considers that the electricity flows from the grid towards the users. In other words, the users can adjust their demand, but not sell back to the grid any energy stored in the battery or produced by the solar panels.

3.1. Similarity to the Lot-Sizing Problem

In a general way, determining the consumption plan under these conditions resembles a classical manufacturing problem: the lot sizing (LS) problem. LS determines the lot sizes that minimize the operational cost of a production process over a multiperiod horizon [26]. We must determine the amount of energy to consume, store and shift in each time frame.

The LS structure allows us to handle the inventory coordination requirement derived from multiple consumers (similar to multiple products). Although the battery is shared among all the users, each user has an individual state of charge.

Additionally, each user has maximum consumptions C^L and C_j^H and is willing to shift load according to the preference parameters Y_j and $\hat{Y}_j$. This is similar to capacitated LS with backlogging [26], where the objective is to minimize the sum of the production, storage, and backlogging costs. The latter helps to represent the load shifting and therefore the demand satisfaction. The variable y_{jt} accounts for both, the amount of unmet demand and the time that demand has remained unmet. We assess the cost of shifting load by solving a biobjective optimization problem via compromise programming.

3.2. Compromise Programming

As mentioned in Section 2, there are different ways to solve a multiobjective optimization problem. All of them seek a trade-off between the conflicting objectives. This is normally represented in the criterion space, which is an image of the feasible set of the optimization problem in terms of the objective functions. Figure 2 shows the Pareto front (dashed red line), the feasible region (gray area), and the two objectives to be minimized (f_1 and f_2).
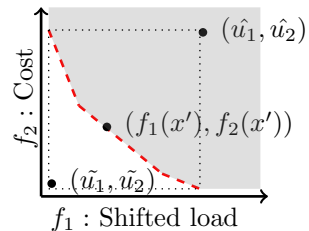

Figure 2: Generic description of criterion space.

The ideal or utopia point $(\tilde{u}_1, \tilde{u}_2)$ is a point where all the objectives achieve their individual optima. Since the objectives conflict, the utopia point is infeasible. Therefore, we want to find a point on the Pareto front that is a fair approximation of the utopia point. Compromise programming finds a Pareto-efficient solution x' that minimizes the Euclidean distance with respect to the utopia point [15]. This process does not require to assign weights and it ensures a unique solution for convex Pareto fronts. The optimization model can easily be adapted to other approaches such as e-constraint and normal boundary intersection, if a representation of the Pareto front is required.

We are dealing with objectives with different units and different orders of magnitude, so it is necessary to normalize their values. We use the nadir point $(\hat{u}_1, \hat{u}_2)$ and the utopia point for the normalization. The nadir point represents the worst value (maximum in this case) of each objective function in the set of nondominated points. The nadir and the utopia points provide respectively tight upper and lower bounds on the nondominated solution set (dotted lines in Figure 2).

We follow these steps to find the compromise solution. First, we solve the optimization problem for each of the individual objectives to compute $\tilde{u}_1$ and $\tilde{u}_2$. We then use the optimal solutions to compute $\hat{u}_1$ and $\hat{u}_2$. Finally we solve a mixed binary quadratic optimization problem to find the closest feasible point to the utopia point. This approach allows us to find a trade-off between the two objectives without approximating the complete Pareto front. Moreover, the objective function remains convex, so the full problem can be solved efficiently by off-the-shelf solvers.

3.3. Optimization Model

The objective function in equation (1) minimizes the squared distance to the utopia point. Equations (2) and (3) account for the shifted load and the total cost respectively. Equation (3) includes the cost of the energy bought from the grid, the cost of using the battery and solar panels, and the incentive paid to the end-users for the DR requests.

$$\min_f \quad \left(\frac{f_1 - \tilde{u}_1}{\hat{u}_1 - \tilde{u}_1}\right)^2 + \left(\frac{f_2 - \tilde{u}_2}{\hat{u}_2 - \tilde{u}_2}\right)^2 \tag{1}$$

$$f_1 = \sum_{j \in J} \sum_{t \in T} y_{jt} \tag{2}$$

$$f_2 = \sum_{i \in I} \sum_{j \in J} \sum_{t \in T} K_{it} x_{ijt} + \sum_{j \in J} \sum_{t \in T} B s_{jt}^+ \\ + \sum_{j \in J} \sum_{t \in T} F g_{jt} - \sum_{j \in J} \sum_{t \in T} L_t r_{jt} \tag{3}$$

Next, we introduce the constraints. Constraints (4) and (5) account for the shifting preferences. In (4) we enforce the maximum accumulated shifted load for each user j throughout the time horizon. Through (5) each user is able to specify the maximum acceptable unmet demand at the end of the horizon (n represents the last time frame). In other words, a user can be flexible about when the demand is satisfied but strict about having it met by the end of the day.

$$\sum_{t \in T} y_{jt} \leq Y_j \qquad \forall \ j \in J \tag{4}$$

$$y_{jn} \leq \hat{Y}_j \qquad \forall \ j \in J \tag{5}$$

The maximum amount of energy that can be drawn from the grid is shown in constraints (6) and (7).

$$x_{1jt} \leq C^L \qquad \forall \ j \in J, \ \forall \ t \in T \tag{6}$$

$$x_{2jt} \leq C_j^H \qquad \forall \ j \in J, \ \forall \ t \in T \tag{7}$$

The parameter C^L is defined by the grid and is given to all the users to ensure a minimal operation. On the other hand, C_j^H depends on each user and represents a large constant from the optimization point of view; we will revisit this definition in Section 4.1.

Constraints (8) and (9) limit the capacity of the solar panels and the battery respectively (battery expressed as a percentage of S^{max}).

$$\sum_{j \in J} g_{jt} \leq G_t^{max} \qquad \forall \ t \in T \tag{8}$$

$$\sum_{j \in J} soc_{jt} \leq 1 \qquad \forall \ t \in T \tag{9}$$

The flow conservation is represented in a similar way to that of LS. Constraint (10) ensures that the inflows and outflows are balanced at every time step. It differs from LS in that it accounts for the efficiency Γ of the battery, which depends on the actual flow of energy and not on the state of charge.

$$\sum_{i \in I} x_{ijt} + g_{jt} + y_{jt} + \Gamma s_{jt}^- \\ = y_{jt-1} + D_{jt} + s_{jt}^+ \quad \forall \ j \in J, \ \forall \ t \in T \tag{10}$$

A common feature of LS is the presence of Wagner–Whitin costs. This cost structure favors production at the time of the demand. The use of storage or the backlogging of orders is penalized; this is traditionally the ideal scenario in manufacturing processes. Wagner–Whitin costs normally simplify the modeling stages in LS because they discard solutions that are suboptimal and do not make sense in a realistic scenario. We use TLOU pricing rather than Wagner–Whitin costs; an analysis of our cost scheme is presented in Section 4. Moreover, we penalize backlogging through the biobjective approach without a specific monetary cost. We include constraint (11) to avoid charging the battery with backlogged load; it describes the physical energy flow toward the battery.

$$g_{jt} + \sum_{i \in I} x_{ijt} - s_{jt}^+ \geq 0 \qquad \forall \ j \in J, \ \forall \ t \in T \tag{11}$$

Constraints (12)–(15) model the operation of the battery. Note that although the model registers every user transaction involving the battery (s_{jt}^+, s_{jt}^-), the cycles are constrained for the whole battery (i.e., the aggregated behavior of the $|J|$ users determines the battery use).

$$soc_{jt} = soc_{jt-1} + \frac{s_{jt}^+ - s_{jt}^-}{S^{max}} \quad \forall \ j \in J, \ \forall \ t \in T \tag{12}$$

$$S^{max}(\alpha_t - 1) \leq \sum_{j \in J}(s_{jt}^+ - s_{jt}^-) \leq S^{max}\alpha_t \quad \forall \ t \in T \tag{13}$$

5

$$-\alpha_t + \alpha_{t-1} \le z_t \qquad \forall \ t \in T \qquad (14)$$

$$\sum_{t \in T} z_t \le Z \qquad (15)$$

Constraint (12) updates the individual state of charge of each user. This value represents the amount of energy in the shared battery available to the user at every time step. Constraint (13) records the events when the battery (as a whole) charges or discharges. Constraints (14) and (15) limit the number of cycles. Note that these constraints do not differentiate between full and partial cycles. The parameter Z is a policy adopted by the building, and the optimization model will determine the type of cycle as a function of the cost and satisfaction. Section 4.4 shows how increasing Z affects the final number and type of cycles.

Solving a biobjective problem for the building does not mean that each user will profit in a similar way from the shared resources. Constraints (16) and (17) ensure a proportional use of the shared resources with respect to the total demand of each user.

$$\Psi_{sol}^{min} \sum_{t \in T} D_{jt} \le \sum_{t \in T} g_{jt} \le \Psi_{sol}^{max} \sum_{t \in T} D_{jt} \quad \forall \ j \in J \quad (16)$$

$$\Psi_{bat}^{min} \sum_{t \in T} D_{jt} \le \sum_{t \in T} soc_{jt} \times S^{max} \le \Psi_{bat}^{max} \sum_{t \in T} D_{jt} \quad \forall \ j \in J \quad (17)$$

Since $\sum_{t \in T} g_{jt} \le \sum_{t \in T} D_{jt}$ (i.e., a housing unit cannot use more solar energy than its total demand), $\Psi_{sol}^{max} \le 1$. An important assumption for the performance of the planning module is that the aggregated demand is always greater than the potential solar generation. This is justified by the building configuration: there are multiple housing units and limited space for roof-mounted panels. If we discarded this assumption, the optimization model could be adapted to absorb the excess solar generation into the battery or to sell it to the energy provider.

The parameter Ψ_{bat}^{max} has a different interpretation. The variable soc_{jt} tells us the level of energy in the battery for each user j and time frame t. For example, if the user charges $1\,\text{kWh}$ at $t = 1$ and keeps it in the battery until $t = 10$, then $soc_{j1}, soc_{j2}, \ldots, soc_{j10} = 1\,\text{kWh} \ /S^{max}$. The summation over these periods will be $10\,\text{kWh}$ of *occupied* battery, regardless of the total demand. In this sense Ψ_{bat}^{max} can be > 1 but still represent fairness as a function of total demand (a user with larger demand can charge the battery with more energy or keep the battery busy for longer). The selection of the upper limits Ψ_{bat}^{max} and Ψ_{sol}^{max} must consider historical demand profiles and capacities to ensure proper utilization of the resources while encouraging their fair allocation.

For the lower bounds Ψ_{bat}^{min} and Ψ_{sol}^{min} it is necessary to ensure feasibility, so they should satisfy

$$\Psi_{bat}^{min} \sum_{j \in J} \sum_{t \in T} D_{jt} \le S^{max} \times |T|$$

and

$$\Psi_{sol}^{min} \sum_{j \in J} \sum_{t \in T} D_{jt} \le \sum_{t \in T} G_t^{max}.$$

We discuss the fair allocation of resources in Section 4.5.

Constraints (18) and (19) account for the building response in the case of a DR request:

$$\sum_{j \in J} r_{jt} = DR_t \phi_t \quad \forall \ t \in T \qquad (18)$$

$$x_{1jt} + x_{2jt} \le (C^L + C_j^H)(1 - \phi_t) + D_{jt}\phi_t - r_{jt} \quad \forall \ j \in J, \forall \ t \in T \qquad (19)$$

If the building agrees to provide DR, each user j will limit his/her consumption to the forecast demand. Additionally, the willing participants contribute r_{jt} units to the grid's load reduction requirement.

Constraint (19) allows the users to reduce their consumption below C^L. If $D_{jt} - r_{jt} \le C^L$ the consumption will stay within the capacity available at a lower tariff. If $C_j^H + C^L \ge D_{jt} - r_{jt} \ge C^L$ the user will consume C^L units at the lower tariff and the additional energy at the higher tariff.

Finally, constraints (20) and (21) are the nonnegativity and binary constraints:

$$x, y, soc, s^+, s^-, g, r, \lambda \ge 0 \qquad (20)$$

$$\alpha_t, z_t, \phi_t \in \{0, 1\}, \quad \forall \ t \in T \qquad (21)$$

3.4. Performance Measures

We use the peak reduction (PR) index and the battery use (BU) as measures of performance:

$$PR = \left(1 - \frac{\max\limits_{t \in T} \sum\limits_{i \in I} \sum\limits_{j \in J} x_{ijt}}{\max\limits_{t \in T} \sum\limits_{j \in J} D_{jt}} \right) \times 100\% \qquad (22)$$

$$BU = \frac{\sum\limits_{t \in T} \sum\limits_{j \in J} soc_{jt}}{|T|} \times 100\% \qquad (23)$$

Although these performance measures are not included in the optimization model, they are important assessments of the operation of the building, and they are reported for all our experiments. These measures could also be used to select efficient solutions in the case where we approximate the Pareto front.

4. Computational Experiments

We carried out various tests to assess the impact of different conditions on the final results. In Section 4.1 we present a base instance (identified with ∗) to illustrate the results obtained with this approach. In subsequent sections we present the results of our sensitivity analysis. In Section 4.2 we explore how the peak reduction is affected by the parameters K_{it}, C^L, and C_j^H. In Section 4.3 we change the end-user willingness to shift load to see the evolution of the Pareto front and to estimate the expected consumer benefit of participating in this type of collaborative scheme. In Section 4.4 we analyze the relationship between the aggregated scheme and the operation of the battery and its cycles. Finally, in Section 4.5 we explore several options for the fair allocation of resources. Since in this case the time frames represent hours, there is a direct equivalence between power (kW) and energy (kWh).

4.1. Base Instance

This instance, which has realistic parameters, includes the following conditions:

- The demand profiles D_{jt} are obtained from *Desimax* [27]. Ten profiles ($|J| = 10$) were chosen for four-person households and were adjusted to the Canadian context, where heating represents around 60% of demand in winter [28]. The daily average energy consumption is 32.5 kWh per user.

- The battery capacity is $S^{max} = 15$ kWh, with a power capacity of 15 kW. The efficiency is $\Gamma = 90\%$, and the number of cycles is $Z = 2$. This battery is similar to the pole-mounted battery from *eCamion* in the context of the *NSERC Energy Storage Technology Network*. It is designed to facilitate the integration of energy management systems.

- There is a solar panel array of $75\,m^2$ with an average daily generation of 34.8 kWh. The daily generation is computed with a historical average solar radiation of $3.45\,kWh/m^2/day$ (Montreal in winter), and a capacity factor of 13.5% [29]. The parameter G_t^{max} is accordingly defined with a peak generation of 4 kWh.

- While $Y_j = \{10, 15, 5, 10, 10, 20, 15, 10, 0, 0\}$, $\hat{Y}_j = 0 \quad \forall j \in J$. The planning horizon has 24 time frames: $T = \{1, \dots, 24\}$.

- The on-peak periods are $t \in \{8, 9, 10, 11, 17, 18, 19\}$, the mid-peak periods are $t \in \{12, \dots, 16\}$, and the off-peak periods are $t \in \{1, \dots, 7, 20, \dots, 24\}$.

- There are six periods in which the building can meet a DR request of 10 kWh.

- The lower capacity $C^L = 1.5$ kW and

$$C_j^H = \max_{t \in T}(0, D_{jt} - C^L), \quad \forall \; j \in J. \qquad (24)$$

This allows each user to consume up to the reported peak demand in any time frame. The initial values y_{j0}, soc_{j0}, and α_0 are 0.

Figure 3 shows the results for the base instance, obtained by solving the optimization model. Figure 3(a) shows that the consumption from the grid differs considerably from the original demand curve. A peak reduction of 13.9% ($t = 18$ on the blue curve versus $t = 20$ on the yellow curve) is achieved by a combination of solar resources, battery, and willingness to shift load. The battery is fully charged at $t = 7$ and $t = 16$, which are the time frames preceding the on-peak time frames. This generates a BU of 47.1%.
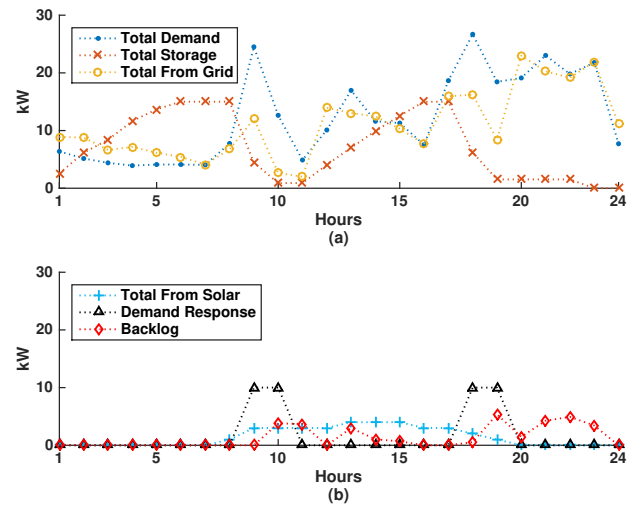

Figure 3: Results for the building in the base instance.

Figure 3(b) shows that the users willing to shift demand make their contribution during the congested periods and consume their requirement by the end of the day. Additionally the building chooses to respond to 4 of 6 DR calls. We can see the reduction of 10 kW in time frames 9, 10, 18, and 19, between the blue (total demand) and the yellow (total from grid) curves in Figure 3(a).

4.2. Cost Structure

The cost structure defined by K_{it}, B, and F determines some of the decisions made by the model. First, the cost F derived from the amortization of the solar panels should be lower than any price we can obtain from the grid. This renewable resource will be utilized first, leaving a net demand curve to be met by using the grid, storage, and load shifting.

As mentioned previously, K_{it}, C^L, and C_j^H are set by the utility. Since there is no direct peak control by the utility, these parameters represent a way to influence the user's consumption profile. Each time frame t belongs to one of three classes: on-peak, mid-peak, or off-peak. For each class the user pays either the *lower* or the *higher* price, depending on the level of consumption. Figure 4

7

	Off-Peak	Mid-Peak	On-Peak
Higher	K_H^{off}	K_H^{mid}	K_H^{on}
Lower	K_L^{off}	K_L^{mid}	K_L^{on}

Figure 4: Energy price policy.

shows a basic representation of the TLOU pricing policy.

We know that $K_H^{off} > K_L^{off}$, $K_H^{mid} > K_L^{mid}$, $K_H^{on} > K_L^{on}$, $K_L^{on} > K_L^{mid} > K_L^{off}$, and $K_H^{on} > K_H^{mid} > K_H^{off}$. In this section we establish some rules to determine how those costs can help to achieve the desired effect in the results. This analysis also includes the battery cost B, which we assume is obtained from cost amortization, and the willingness of the users to shift load.

Equations (25) and (26) show two possible cost structures for a cheaper and a more expensive period (off-peak and on-peak). The following reasoning can be extended to the other combinations: off-peak and mid-peak, and mid-peak and on-peak.

$$K_L^{off} + B < K_L^{on} < K_H^{off} + B < K_H^{on} \qquad (25)$$

$$K_L^{off} + B < K_H^{off} + B < K_L^{on} < K_H^{on} \qquad (26)$$

A cost structure based on equation (25) will encourage consumption of energy from the lower capacities before going to the higher level. On the other hand, a cost structure based on equation (26) will encourage using all the off-peak resources before moving to more expensive time frames.

The selection of the cost structure is key for the decision making in two specific circumstances:

1. The user shifts load from the on-peak to the future off-peak periods. In this case the battery cost is not included (i.e., $B = 0$).

2. The user wants to charge the battery in the off-peak time frames to use the energy in the later on-peak periods. Here the battery cost $B > 0$ is considered.

Table 1 reports the results for both cost structures. The parameter C^L increases by $0.5\,\text{kWh}$ from one instance to the next.

First, observe that the BU is similar in every case; it depends on the capacity of the battery and the number of time frames where using the battery makes sense.

Observe also that the instances with equation (25) report a better PR. In fact, the peak demand increases considerably for the instances with equation (26). Figure 5 shows the results for instance 6. In this case the cost structure based on equation (26) encourages a very high load shifting from time frame 19 (on-peak) to time frame 20 (off-peak), since it is always cheaper to consume in off-peak periods regardless the consumption level.

Table 1: Comparison of cost structures and available capacities

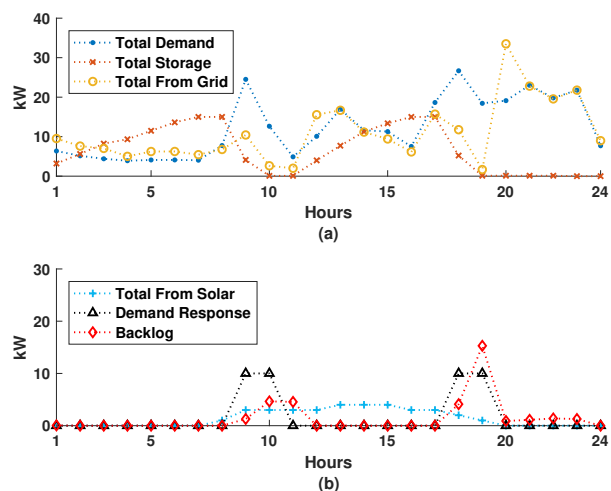| Inst	K_{it}	C^L	f_1	f_2	PR	BU
1	(25)	1.0	31.0	2973.9	-0.8	44.7
2*	(25)	1.5	32.2	2750.4	13.9	47.1
3	(25)	2.0	33.7	2615.0	10.2	47.1
4	(25)	2.5	33.4	2535.3	-1.6	49.1
5	(26)	1.0	34.6	2703.4	-46.5	42.9
6	(26)	1.5	34.6	2605.6	-25.7	47.1
7	(26)	2.0	34.0	2543.3	-10.6	47.1
8	(26)	2.5	34.0	2499.8	-17.5	43.8

Figure 5: Results for the building in the instance 6 of cost analysis.

In general terms, equation (25) leads to a more homogeneous use of the available capacities, where energy is first consumed in the lower levels regardless of the time of use.

Of the experiments with equation (25), instances 2* and 3 achieve better PR; the peak slightly increases in instances 1 and 4. A low C^L will be consumed quickly and the shiftable demand will accumulate in the higher level of the cheapest time frames. A large C^L will render the higher level useless and will accumulate the shiftable demand in the lower level of the cheapest time frames. In both cases we basically move the peak from an expensive period to a cheaper one. Figure 6 shows the peak reduction as a function of C^L using the costs in (25). We see that the PR is positive for only a small range of C^L, approximately 1.1 to 2.4.

It is important to recall that PR is not considered in the optimization problem, and our approach achieves the PR as an additional effect. Nevertheless, our discussion can guide future decisions about how to determine the capacity profiles.
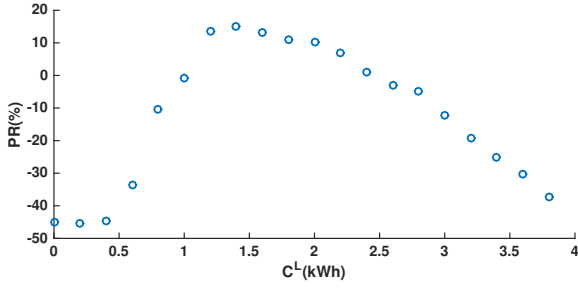
8

Figure 6: Peak reduction as a function of C^L.

4.3. Willingness to Participate

In this section we show how the end-user willingness to shift load affects the results. We change the parameter Y_j in each instance in Table 2. In instance 1 the users are more willing to shift load, and in instance 5 the users prefer not to change their consumption patterns.

Table 2: Results for different populations

Inst	$\tilde{u}_1$	$\tilde{u}_2$	f_1	f_2	PR	BU	Φ
1	0.0	2632.1	51.0	2703.5	17.2	47.1	4/6
2*	0.0	2678.2	32.2	2750.4	13.9	47.1	4/6
3	0.0	2774.2	10.1	2816.4	14.6	46.8	4/6
4	0.0	2838.1	3.2	2854.4	16.4	49.7	3/6
5	0.0	2873.2	0.5	2876.0	13.7	46.5	2/6

The utopian value $\tilde{u}_1$ remains the same while $\tilde{u}_2$ increases as the willingness to shift load reduces. The compromise solution (f_1, f_2) becomes closer to the utopia point. The evolution of the Pareto front is shown in Figure 7.
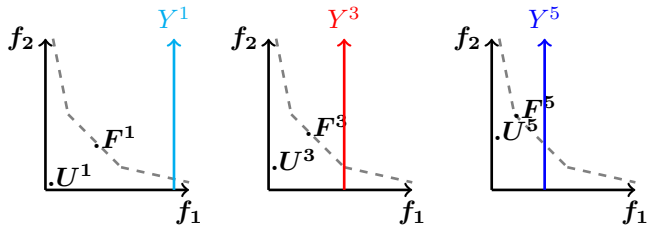

Figure 7: Evolution of the Pareto front.

Y^{inst}, F^{inst}, and U^{inst} represent the aggregated willingness, the compromise solution, and the utopia point for each instance respectively. The BU has similar behavior to that in Section 4.2.

Although we achieve PR in all the instances, the behavior with respect to Y_j is not clear: Y_j can generate a higher or lower PR depending on the selection of C^L and the prices.

In the last column we introduce the ratio Φ, which is defined to be the total number of DR calls accepted by the building divided by the potential DR requests. As the willingness to shift load decreases the building responds to

fewer DR requests. Figure 8 shows the results for instance 5. In this instance the users are not willing to shift load, therefore the backlogged demand is zero. Additionally, we can see how the building can only provide DR reduction in time frames 9 and 18.
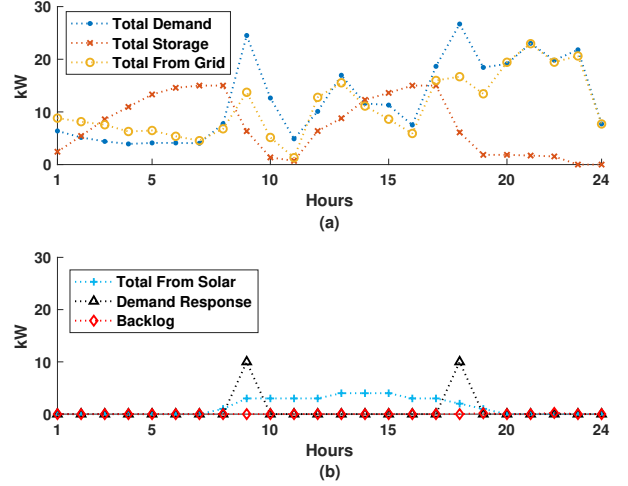

Figure 8: Results for the building in the instance 5 of user willingness.

Table 3 gives the individual cost per user and instance. Typically, the more willing the user is to shift load the lower the total cost. In the last column we compute the total cost for a scenario Ω without the collaborative approach. In this case there are no resources (storage, solar panels, or DR incentives). The users meet their demands as they occur, paying the same price rates K_{it}. The last row of the table shows the average savings (Sav) with respect to the scenario Ω.

Table 3: Total cost per housing unit

User	Inst1	Inst2	Inst3	Inst4	Inst5	Ω
1	177.4	179.9	181.3	183.1	183.1	211.6
2	328.6	341.7	352.3	363.9	357.8	446.5
3	278.0	286.6	308.3	282.7	284.0	453.9
4	301.4	305.6	309.8	315.4	323.0	412.8
5	203.6	206.6	210.0	213.0	213.0	251.3
6	384.9	383.3	427.2	422.5	433.6	529.4
7	216.1	216.7	218.2	223.4	223.1	276.2
8	270.8	271.8	251.8	288.3	296.4	357.4
9	238.0	248.4	247.7	248.0	248.0	278.8
10	304.8	309.9	310.0	314.2	314.0	369.0
Sav	25.0%	23.3%	21.4%	20.3%	19.7%	0%

One of the key assumptions of this work is that the parameters B and F, representing the amortization costs of the battery and the solar panels, must be lower than the rates that come from the grid or the building operator. Therefore, the collaboration allows the user to take advantage of resources that would be more expensive to

own individually. In general terms, the more willing the user is to shift load, the lower the total cost will be. However, this statement is not necessarily true. A willing user may not be asked to shift load; this depends on the global benefit that the shifting provides to the community (because the model gives priority to users that can shift load from on-peak periods).

4.4. Battery Cycles and Aggregation

One of the most common issues with storage units is the proper use of the resource to minimize its degradation. Although in this paper we assume an amortization cost to take this into account, we also included constraints to control the number of cycles. The results for different values of Z are presented in Table 4.

Table 4: Results for different maximum number of cycles

Inst	u_1	u_2	f_1	f_2	PR	BU	z/Z
1	0.0	2708.6	35.1	2789.3	13.9	52.7	1/1
2*	0.0	2678.2	32.2	2750.4	13.9	47.1	2/2
3	0.0	2678.2	32.1	2750.4	13.9	47.1	3/3
4	0.0	2678.2	32.1	2750.4	13.9	47.1	3/6
5	0.0	2678.2	32.1	2750.4	13.9	47.1	3/12

We observe that the number of cycles is fairly stable at $z = 3$, giving the same compromise solution regardless of the value of Z. What happens is that the number of cycles is determined by the cost structure in combination with the user demand. There are only some periods where it is sensible to use the battery: charge in the current (cheaper) frame to discharge in a future (more expensive) one. Note that the model will work even when the cycles constraints are removed. On the other hand, there are some cases when it is convenient to monitor the number of cycles. For example when the demand profiles change considerably from user to user, or when the prices vary in a real time context.

4.5. Allocation of Resources

In Section 3.3 we introduced the fair allocation of the shared resources with constraints (16) and (17). In this section we assess the effect of this on the objective function. We test three models (the original and two variations). In the first we do not include a fairness constraint; in the second we include the original constraints (16) and (17); and in the third we include constraints (27) and (28) instead:

$$\sum_{t \in T} g_{jt} - \sum_{t \in T} g_{j-1t} = 0 \qquad \forall \ j \in J \mid j > 1 \qquad (27)$$

$$\sum_{t \in T} soc_{jt} - \sum_{t \in T} soc_{j-1t} = 0 \qquad \forall \ j \in J \mid j > 1 \qquad (28)$$

Constraint (27) ensures that all the users obtain the same amount of energy from the solar panels. In a similar way, constraint (28) ensures that all the users have the same accumulated state of charge over the time horizon (i.e., the battery is equally utilized). We report the results in Table 5. Although the three models report the same $u_1 = 0$, they have different u_2 values. Model 1 gives the lowest u_2 since no constraints related to fair allocation were considered, giving priority to the overall cost for the building. On the other hand, Model 3 reports the highest u_2 because enforcing the same amount of resources for each user is inefficient when the users have significantly different consumption profiles. These utopia values affect the compromise solution f_1 and f_2 as explained in Section 3.2.

Table 5: Results for different fairness constraints

Model	u_1	u_2	f_1	f_2
1	0.0	2665.2	33.3	2733.0
2*	0.0	2678.2	32.2	2750.4
3	0.0	2695.6	32.0	2767.6

Figure 9 presents more detailed results for each user. Figure 9(a) shows the solar allocation expressed as a percentage of the demand ($\sum_{t \in T} g_{jt} / \sum_{t \in T} D_{jt}$). Figure 9(b) shows the battery allocation ($\sum_{t \in T} soc_{jt} \times S^{max} / \sum_{t \in T} D_{jt}$), and Figure 9(c) gives the shifted load as a percentage of the total shiftable load ($\sum_{t \in T} y_{jt} / Y_j$).
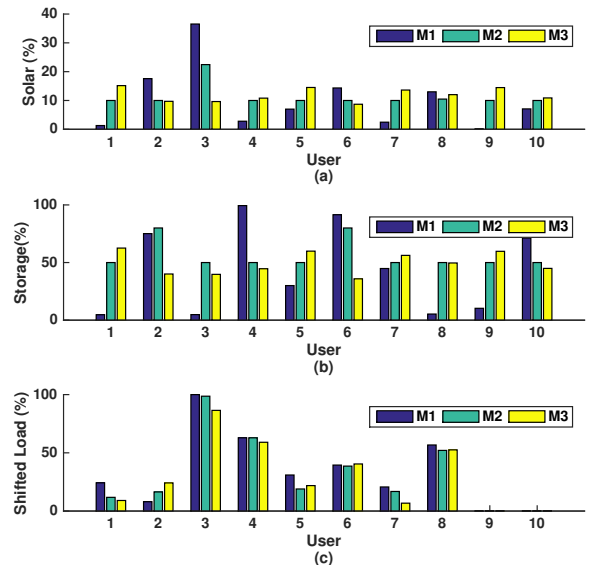

Figure 9: Comparison of allocation of resources per user. Solar and battery are expressed as a percentage of the demand, and shifted load is expressed as a percentage of the total shiftable load.

The percentages for model 1 vary considerably among the users in Figures 9(a) and (b). The percentages for

model 3 vary as a function of the individual user demand in Figures 9(a) and (b). Finally, model 2 enforces $\Phi_{sol}^{min} = 10\%$ and $\Phi_{bat}^{min} = 50\%$ in Figures 9(a) and (b) respectively, providing a more balanced allocation of the resources.

In Figure 9(c) we can see that the amount of shifted load does not change significantly with the selection of the model. As mentioned in Section 4.3, the optimal load shifting depends on being able to shift load at the right moment during the day. In other words, user 3 with $Y_3 = 5$ can be asked to shift near 100% of his shiftable load, while user 5 with $Y_5 = 10$ is just shifting about 20%. This could lead to another form of fair allocation of resources since it makes sense that the users that contribute more to the building performance can obtain a larger share of the resources in order to minimize their individual costs.

5. Conclusion

The approach presented in this work contributes to the planning and operation of smart buildings. It has a structure similar to that of classic LS, but it supports decision-making in the context of energy consumption for a multi-unit building. We address two conflicting objectives, cost and comfort, via the compromise solution. The proposed approach balances the two objectives while providing demand response to the grid. This is possible because of the combination of the available resources (solar and storage), active user participation, and a cost structure that provides incentives for load shifting and peak reduction.

We presented a detailed analysis of the effect of the different parameters on the compromise solution. First, we introduced a base instance that reports around 23% cost savings for the users and a PR of 13.9%. Then, we assessed four cases in which we changed the parameters or the model. In the first case, we explored how the cost structure affects the PR. In the second case, we see that users more willing to participate can obtain more cost savings. In the third case, we show that the number of battery cycles depends on the demand profiles and the cost structure. Finally, we see that a fair allocation of resources among the users reduces the global performance of the building but may facilitate future user participation in the program.

This analysis provides insights into the conditions needed to ensure the long-term operation and economic viability of the approach for the building and the individual users. The proposed approach is applicable in practice because, as discussed in Section 3, the necessary technology is already available. Nevertheless, we acknowledge that there are necessary conditions to be satisfied before successfully implementing this approach. First, the technology should be affordable or the savings for the user should be enough to justify the investment in the technology. Second, the utility has to define the prices and capacities of TLOU in such a way that the TLOU is operationally effective for the utility and attractive enough for the end-users. This is not a trivial task and is currently the subject of ongoing research. Finally, most of the decisions on the user side have to be made in an automatic way. This automation, combined with the potential economical benefits, would likely ensure user engagement with the program.

References

[1] D. Kathan, R. Aldina, M. P. Lee, L. Medearis, P. Sporborg, M. Tita, D. Wight, W. A., Assessment of Demand Response and Advanced Metering, Department of Energy, Washington, DC.

[2] P. Siano, Demand response and smart grids: A survey, Renewable and Sustainable Energy Reviews 30 (2014) 461–478.

[3] Electric Power Annual 2014, Tech. rep., U.S. Energy Information Administration, Washington, DC (2016).

[4] A. Parisio, E. Rikos, L. Glielmo, A model predictive control approach to microgrid operation optimization, IEEE Transactions on Control Systems Technology 22 (5) (2014) 1813–1827.

[5] P. O. Kriett, M. Salani, Optimal control of a residential microgrid, Energy 42 (1) (2012) 321–330.

[6] R. Palma-Behnke, C. Benavides, F. Lanas, B. Severino, L. Reyes, J. Llanos, D. Saez, A microgrid energy management system based on the rolling horizon strategy, IEEE Transactions on Smart Grid 4 (2) (2013) 996–1006.

[7] D. ce Gao, Y. Sun, Y. Lu, A robust demand response control of commercial buildings for smart grid under load prediction uncertainty, Energy 93 (2015) 275 – 283.

[8] S. Mhanna, A. C. Chapman, G. Verbič, A fast distributed algorithm for large-scale demand response aggregation, IEEE Transactions on Smart Grid 7 (4) (2016) 2094–2107.

[9] P. Mesaric, S. Krajcar, Home demand side management integrated with electric vehicles and renewable energy sources, Energy and Buildings 108 (2015) 1–9.

[10] T. AlSkaif, A. C. Luna, M. G. Zapata, J. M. Guerrero, B. Bellalta, Reputation-based joint scheduling of households appliances and storage in a microgrid with a shared battery, Energy and Buildings 138 (2017) 228–239.

[11] A. Chabaud, J. Eynard, S. Grieu, A new approach to energy resources management in a grid-connected building equipped with energy production and storage systems: A case study in the south of France, Energy and Buildings 99 (2015) 9–31.

[12] K. P. Detroja, Optimal autonomous microgrid operation: A holistic view, Applied Energy 173 (2016) 320–330.

[13] A. A. Hasib, N. Nikitin, L. Natvig, Cost-comfort balancing in a smart residential building with bidirectional energy trading, in: 2015 Sustainable Internet and ICT for Sustainability (SustainIT), 2015, pp. 1–6.

[14] M. Ehrgott, Multicriteria Optimization, Springer Science & Business Media, 2006.

[15] R. T. Marler, J. S. Arora, Survey of multi-objective optimization methods for engineering, Structural and Multidisciplinary Optimization 26 (6) (2004) 369–395.

[16] R. Yang, L. Wang, Multi-objective optimization for decision-making of energy and comfort management in building automation and control, Sustainable Cities and Society 2 (1) (2012) 1–7.

[17] X. Zhang, R. Sharma, Y. He, Optimal energy management of a rural microgrid system using multi-objective optimization, in: 2012 IEEE PES Innovative Smart Grid Technologies (ISGT), 2012, pp. 1–8.

[18] V. Hosseinnezhad, M. Rafiee, M. Ahmadian, P. Siano, Optimal day-ahead operational planning of microgrids, Energy Conversion and Management 126 (2016) 142–157.

[19] J. Aghaei, M.-I. Alizadeh, Multi-objective self-scheduling of CHP (combined heat and power)-based microgrids considering demand response programs and ESSs (energy storage systems), Energy 55 (2013) 1044–1054.

[20] M. Choobineh, S. Mohagheghi, A multi-objective optimization framework for energy and asset management in an industrial microgrid, Journal of Cleaner Production 139 (2016) 1326–1338.

[21] X. Cao, J. Wang, Z. Zhang, Multi-objective optimization of preplanned microgrid islanding based on stochastic short-term simulation, International Transactions on Electrical Energy Systems 27 (1).

[22] C. D. Korkas, S. Baldi, I. Michailidis, E. B. Kosmatopoulos, Occupancy-based demand response and thermal comfort optimization in microgrids with renewable energy sources and energy storage, Applied Energy 163 (2016) 93–104.

[23] R. Dai, M. Hu, D. Yang, Y. Chen, A collaborative operation decision model for distributed building clusters, Energy 84 (2015) 759 – 773.

[24] T. K. Hui, R. S. Sherratt, D. D. Sanchez, Major requirements for building smart homes in smart cities based on internet of things technologies, Future Generation Computer Systems 76 (2017) 358 – 369.

[25] J. A. Gomez-Herrera, M. F. Anjos, Optimization-based estimation of power capacity profiles for activity-based residential loads, International Journal of Electrical Power and Energy Systems (2018, to appear).

[26] Y. Pochet, L. A. Wolsey, Production Planning by Mixed Integer Programming, Springer Science & Business Media, 2006.

[27] A. J. Collin, G. Tsagarakis, A. E. Kiprakis, S. McLaughlin, Development of low-voltage load models for the residential load sector, IEEE Transactions on Power Systems 29 (5) (2014) 2180–2188.

[28] Households and the Environment: Energy Use, Tech. rep., Statistics Canada, Ottawa, ON (2013).

[29] N. R. E. Laboratory, Pvwatts calculator, `http://pvwatts.nrel.gov/index.php` (2016).